Enhancing loss modulus of carbon fibre polymer matrix composites by addition of particles in interlaminar region

S. W. Hudnut and D. D. L. Chung

The addition of tin–zinc (Sn–9Zn) particles of size 25–45 μm to a continuous carbon fibre epoxy matrix composite in the interlaminar region has resulted in a hybrid composite containing 10 vol.-% particles and exhibiting a loss modulus of 2 GN m^{-2} and a density of 2·0 g cm^{-3} for a longitudinal flexural specimen. The particle addition increased the loss modulus by >20 000% and the density by 34%. The loss modulus increase was due to an increase in the loss tangent (tan δ), which more than compensated for the decrease in the storage modulus. For a transverse flexural specimen (a configuration that has no practical use), the loss modulus was decreased by the particle addition by about 60%, owing to decreases of both tan δ and the storage modulus.
PRCPA/1213

 The authors are in the Composite Materials Research Laboratory, State University of New York at Buffalo, Buffalo, NY 14260–4400, USA. Manuscript received 24 July 1995; in final form 1 December 1995.

INTRODUCTION

The vibrational damping ability of carbon fibre polymer matrix composites is important in numerous applications, including sporting goods, antisonar submarines, loudspeaker diaphragms, and aerospace structures. Viscoelastic layers (such as rubber) have been incorporated in these composites to increase the damping ability, but they result in large decreases in the modulus and strength of the composite,[1] an increased tendency to delaminate,[2] and a lower maximum service temperature.[3] Metal alloys tend to have a better damping ability than carbon fibre polymer matrix composites, but their densities are usually high. Even aluminium alloys, which are very light, exhibit higher densities than carbon fibre polymer matrix composites. A material having a high damping ability, high modulus, high strength, and low density is required.

The addition of a discontinuous filler rather than a continuous interlayer to a continuous fibre polymer matrix composite has been used to improve some mechanical properties. For example, rubber particles[4] and thermoplastic particles[5] have been added to improve the toughness and impact resistance, as the particles promote multiple cracking and delamination modes.[5] Rigid particles such as alumina, silica, glass beads, and block copolymers, in addition to ceramic whiskers, have been used to increase the strength, stiffness, toughness, and/or fatigue resistance,[5,6] since the additional filler provides crack pinning.[5] Ductile tin–lead alloy particles have been used to increase the fatigue resistance, as the ductile particles between the plies are believed to prevent crack propagation from one ply to another.[7,8] However, the use of discontinuous filler addition to enhance the damping ability or loss modulus has not been addressed previously, except in Refs. 7 and 8, in which the method of damping ability evaluation suffered from poor accuracy. In the present paper, the beneficial effect of ductile alloy particle addition between the plies on the damping ability and loss modulus is reported.

An Sn–40Pb alloy was used in Refs. 7 and 8 because of its ductility and low melting temperature (liquidus 188°C, solidus 183°C), which allowed the alloy particles to melt during the curing of the polymer matrix. Owing to the health and environmental hazards of lead in Sn–40Pb, the present study used Sn–9Zn eutectic alloy (melting temperature 199°C) instead. In contrast to Ref. 4, the alloy particles did not melt during the curing of the polymer matrix.

Table 1 Fibre and matrix properties (according to ICI Fiberite)

10E–Torayca T-300 (6 K) untwisted, UC-309 sized	
Density, g cm^{-3}	1·76
Tensile modulus, GN m^{-2}	221
Tensile strength, GN m^{-2}	3·1
976 Epoxy	
Process temperature, °C	177
Maximum service temperature: dry, °C	177
wet, °C	121
Flexural modulus, GN m^{-2}	3·7
Flexural strength, MN m^{-2}	138
T_g, °C	232
Density, g cm^{-3}	1·28

EXPERIMENTAL METHODS

Sn–9Zn eutectic alloy particles of size 25–45 μm and density 7·26 g cm^{-3} (Indalloy 201, Indium Corporation of America, Utica, NY) were used as the interlaminar discontinuous filler. Composite samples were constructed from individual layers cut from a 12 in* wide unidirectional carbon fibre prepregnated tape manufactured by ICI Fiberite (Tempe, AZ). The product used was Hy-E 1076E, which consisted of a 976 epoxy matrix and 10E graphite fibres. The fibre and matrix properties are given in Table 1.

* 1 in ≡ 25·4 mm.

Table 2 Laminate density and thickness

Laminate type	Laminate density, g cm^{-3}	Laminate thickness, mm
$[0]_8$ and $[90]_8$, no filler	1.53 ± 0.01	0.94
$[0, \pm 45, 90]_s$, no filler	1.56 ± 0.01	0.90
$[0]_8$ and $[90]_8$ with particles	2.04 ± 0.02	1.20
$[0, \pm 45, 90]_s$ with particles	1.96 ± 0.04	1.25

The composite laminates were laid up in a 4 × 7 in platten compression mould with laminate configurations of $[0]_8$, $[90]_8$, and $[0, \pm 45, 90]_s$. The individual 4 × 7 in fibre layers (eight per laminate) were cut from the prepregnated tape. The layers were stacked in the mould with a mould release film on the top and bottom of the layup. A liquid mould release was unnecessary. For laminates with an interlaminar filler, the interlaminar filler material was dispersed across each ply as they were laid up, producing laminates with eight layers of carbon fibres and seven interlaminar regions containing the interlaminar filler. A uniform layer of interlaminar filler material (2·21 g) was ensured since only one monolayer of the filler can adhere to the tacky prepregnated plies. The density and thickness of the laminates are given in Table 2. The thickness of the interlaminar filler layers obtained by calculating the difference between thicknesses of laminates with and without the interlaminar filler, is given in Table 3 for each laminate configuration. The thickness of each carbon fibre layer was 110 µm. The volume fraction of carbon fibres in the composite without the interlaminar filler was 52%; the volume fractions of carbon fibres and of the interlaminar filler in composites having interlaminar filler are also given in Table 3. The laminates were cured using a cycle based on the ICI Fiberite C–5 cure cycle. The curing occurred at 179 ± 6°C and 0·61 MPa for 120 min. After curing, the laminates were cut to give samples of size 25 × 2·5 mm. The $[90]_8$ specimens were cut from the same laminates as the $[0]_8$ specimens.

Dynamic testing of the composite beams was carried out on a Perkin-Elmer dynamic mechanical analyser (DMA7e). The specimens were tested in three point bending (Fig. 1) in the temperature scan mode from 30 to 180°C at frequencies of 0·2, 0·4, 1·0, 2·0, and 4·0 Hz. The heating rate used for all tests was 2 K min^{-1}, which was chosen to prevent any artificial damping peaks that may be caused by higher heating rates. The loads used during testing were all sufficiently large that the amplitude of the specimen deflection was always above the minimum value of 5 µm required by the machine for accurate results. The loads were then set such that each different type of specimen was always tested at its appropriate stress level. The storage modulus (bending modulus) and loss tangent (tan δ) values from each test were then plotted using the attached UNIX workstation.

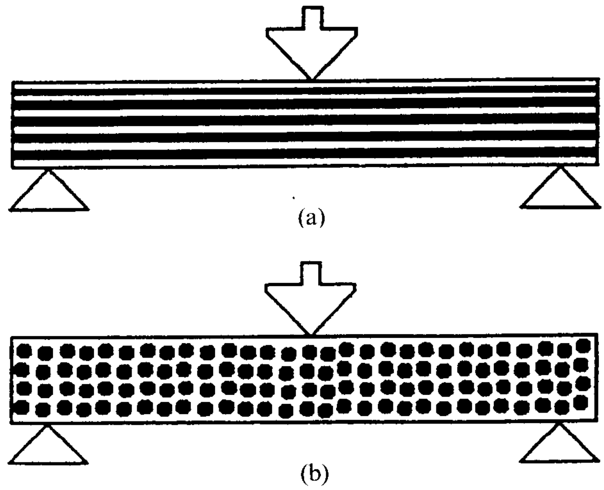

1 Sample configuration for dynamic flexural testing: *a* $[0]_8$ sample (fibres parallel to page); *b* $[90]_8$ sample (fibres perpendicular to page)

RESULTS

Table 4 gives the values of tan δ, storage modulus, and loss modulus at 30°C at various frequencies. Table 5 gives the values at 1·0 Hz and various temperatures. Figures 2–4 show plots of tan δ *v.* temperature at 0·2, 1·0, and 4·0 Hz for the $[0]_8$, $[0, \pm 45, 90]_s$, and $[90]_8$ laminates, respectively, each having interlaminar filler. Figures 5–7 show corresponding plots for storage modulus *v.* temperature. The addition of the interlaminar filler increased tan δ for the $[0]_8$ and $[0, \pm 45, 90]_s$ laminates, but decreased it for the $[90]_8$ laminate. For any combination of temperature and frequency, tan δ was greater for $[90]_8$ than for $[0]_8$ or $[0, \pm 45, 90]_s$ and tan δ was greater for $[0]_8$ than for $[0, \pm 45, 90]_s$, with or without the interlaminar filler. The addition of the interlaminar filler decreased the storage modulus for any laminate configuration and any combination of temperature and frequency. The fractional decrease in modulus due to the interlaminar filler addition was much greater for $[0]_8$ and $[0, \pm 45, 90]_s$ than for $[90]_8$. The modulus was much higher for $[0]_8$ and $[0, \pm 45, 90]_s$ than for $[90]_8$, and was higher for $[0]_8$ than for $[0, \pm 45, 90]_s$, whether the interlaminar filler was present or not. The value

Table 3 Volume fractions of fillers and interlaminar layer thickness

Laminate type	Fibres in composite, vol.-%	Interlaminar filler in composite, vol.-%	Interlaminar filler in interlaminar layer, vol.-%	Interlaminar filler layers in total composite, vol.-%	Thickness of interlaminar filler layers, µm
$[0]_8$ and $[90]_8$ with particles	33·1	10·1	39·0	25·7	44
$[0, \pm 45, 90]_s$ with particles	21·7	9·6	33·8	28·4	51

Table 4 Tan δ, and storage, and loss moduli at 30°C

Frequency, H_2	Tan δ $[0]_8$	Tan δ $[0, \pm 45, 90]_s$	Tan δ $[90]_8$	Storage modulus, GN m^{-2} $[0]_8$	Storage modulus, GN m^{-2} $[0, \pm 45, 90]_s$	Storage modulus, GN m^{-2} $[90]_8$	Loss modulus, GN m^{-2} $[0]_8$	Loss modulus, GN m^{-2} $[0, \pm 45, 90]_s$	Loss modulus, GN m^{-2} $[90]_8$
Without interlaminar filler									
0·2	0·008 ± 0·003	0·006 ± 0·003	0·010 ± 0·003	101 ± 1	76 ± 1	7·9 ± 0·1	0·8 ± 0·3	0·46 ± 0·24	0·079 ± 0·025
1·0	< 0·0001	< 0·0001	0·090 ± 0·005	97 ± 1	71 ± 1	8·3 ± 0·1	< 0·0097	< 0·0071	0·75 ± 0·05
4·0	< 0·0001	< 0·0001	0·050 ± 0·006	103 ± 1	76 ± 1	8·2 ± 0·1	< 0·0103	< 0·0076	0·41 ± 0·05
With interlaminar filler									
0·2	0·042 ± 0·003	0·030 ± 0·003	0·040 ± 0·001	81 ± 1	56 ± 1	7·3 ± 0·1	3·40 ± 0·29	1·68 ± 0·20	0·29 ± 0·01
1·0	0·022 ± 0·001	0·004 ± 0·001	0·047 ± 0·004	78 ± 1	53 ± 1	7·8 ± 0·1	1·72 ± 0·10	0·21 ± 0·06	0·37 ± 0·03
4·0	0·004 ± 0·003	< 0·0001	0·066 ± 0·004	82 ± 1	55 ± 1	8·2 ± 0·1	0·33 ± 0·25	< 0·0055	0·54 ± 0·04

Table 5 Tan δ, and storage, and loss moduli at 1·0 Hz

Temperature, °C	Tan δ $[0]_8$	Tan δ $[0, \pm 45, 90]_s$	Tan δ $[90]_8$	Storage modulus, GN m^{-2} $[0]_8$	Storage modulus, GN m^{-2} $[0, \pm 45, 90]_s$	Storage modulus, GN m^{-2} $[90]_8$	Loss modulus, GN m^{-2} $[0]_8$	Loss modulus, GN m^{-2} $[0, \pm 45, 90]_s$	Loss modulus, GN m^{-2} $[90]_8$
Without interlaminar filler									
30	< 0·0001	< 0·0001	0·090 ± 0·005	97 ± 1	71 ± 1	8·3 ± 0·1	< 0·0097	< 0·0071	0·75 ± 0·05
100	< 0·0001	< 0·0001	0·120 ± 0·008	96 ± 1	70 ± 1	7·8 ± 0·1	< 0·0096	< 0·0070	0·94 ± 0·06
175	< 0·0001	< 0·0001	0·130 ± 0·008	96 ± 1	70 ± 1	7·8 ± 0·1	< 0·0096	< 0·0070	1·0 ± 0·1
With interlaminar filler									
30	0·022 ± 0·003	0·004 ± 0·001	0·047 ± 0·003	78 ± 1	53 ± 1	7·8 ± 0·1	1·72 ± 0·10	0·21 ± 0·06	0·37 ± 0·03
100	0·022 ± 0·003	0·009 ± 0·002	0·045 ± 0·003	75 ± 1	52 ± 1	7·1 ± 0·1	1·65 ± 0·10	0·47 ± 0·11	0·32 ± 0·03
175	0·031 ± 0·003	0·019 ± 0·001	0·047 ± 0·003	71 ± 1	52 ± 1	6·8 ± 0·1	2·20 ± 0·25	0·99 ± 0·07	0·32 ± 0·03

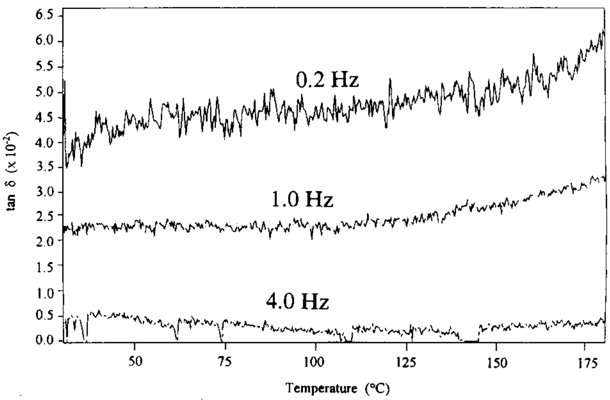

2 Plot of tan δ *v.* temperature at 0·2, 1·0, and 4·0 Hz for $[0]_8$ laminate having interlaminar filler

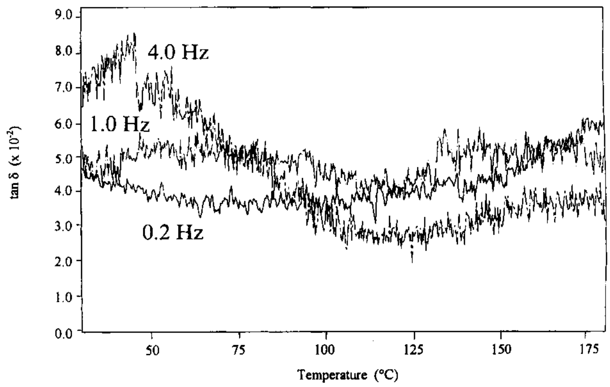

4 Plot of tan δ *v.* temperature at 0·2, 1·0, and 4·0 Hz for $[90]_8$ laminate having interlaminar filler

of tan δ increased with increasing temperature in most instances. The modulus decreased with increasing temperature in most instances. The value of tan δ generally decreased with increasing frequency.

The product of tan δ and the storage modulus is the loss modulus, which is also given in Tables 4 and 5. The addition of the interlaminar filler increased the loss modulus for the $[0]_8$ and $[0, \pm 45, 90]_s$ laminates, but its effect varied for the $[90]_8$ laminate. Despite the decrease in the storage modulus, the increase in tan δ caused the loss modulus to increase for the $[0]_8$ and $[0, \pm 45, 90]_s$ laminates having added interlaminar filler.

Figure 8 shows an optical micrograph of the polished cross-section of the $[0, \pm 45, 90]_s$ laminate having interlaminar filler. The particles (bright circles) were mostly in a monolayer form between the fibre plies. Some of the particles had fallen out during polishing.

DISCUSSION

The flexural behaviour of $[0]_8$ and $[0, \pm 45, 90]_s$ laminates is governed by the fibres, but in the $[90]_8$ laminate it is governed by the matrix. The first two laminates therefore exhibit low tan δ and high storage modulus, while the last exhibits high tan δ and low storage modulus. The combined effects of interlaminar filler addition on tan δ and storage modulus cause the loss modulus to be increased for the $[0]_8$ and $[0, \pm 45, 90]_s$ laminates and either decreased or increased for the $[90]_8$ laminate. The loss modulus is lower for the $[0]_8$ and $[0, \pm 45, 90]_s$ laminates than the $[90]_8$ laminate without interlaminar filler, but is higher for the $[0]_8$ laminate than the $[90]_8$ or $[0, \pm 45, 90]_s$ laminates having interlaminar filler, except for certain combinations of temperatures and frequencies, e.g. 30°C and 4·0 Hz. The fractional increase in loss modulus due to interlaminar filler addition ranges from >17 000% to >23 000% for $[0]_8$ and from >2900% to >14 000% for $[0, \pm 45, 90]_s$, considering all combinations of temperatures and frequencies. The fractional decrease in loss modulus due to interlaminar filler addition ranges from 51 to 68% for $[90]_8$, except for certain combinations of temperature and frequency, e.g. 30°C and 0·2 and 4·0 Hz, for which the loss modulus is decreased by interlaminar filler addition. As the $[0]_8$ and $[0, \pm 45, 90]_s$ laminates, being fibre dominated, are of greater practical value than the $[90]_8$ laminate, the effect of interlaminar filler addition is significant and practically useful.

The decrease in storage modulus due to interlaminar filler addition results from the low storage modulus of the interlaminar filler. The increase in tan δ due to interlaminar filler addition is attributed

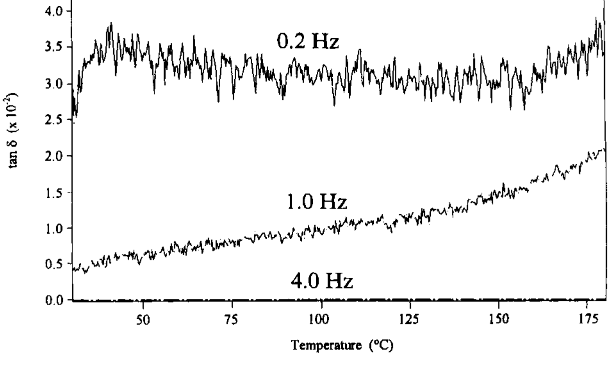

3 Plot of tan δ *v.* temperature at 0·2, 1·0, and 4·0 Hz for $[0, \pm 45, 90]_s$ laminate having interlaminar filler

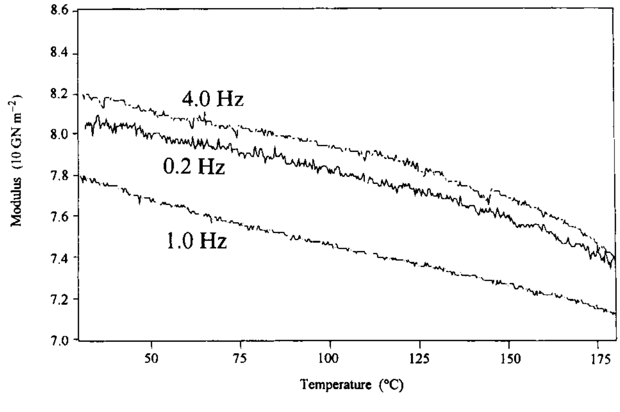

5 Plot of storage modulus *v.* temperature at 0·2, 1·0, and 4·0 Hz for $[0]_8$ laminate having interlaminar filler

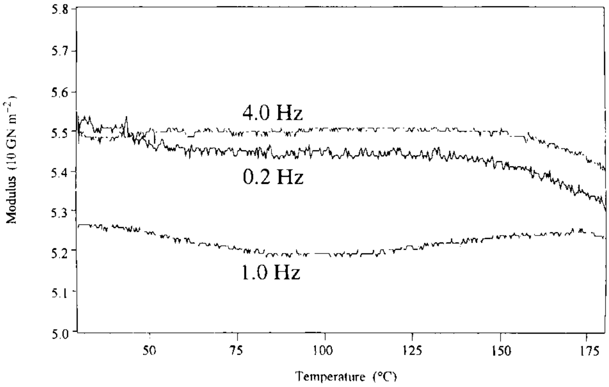

6 Plot of storage modulus *v.* temperature at 0·2, 1·0, and 4·0 Hz for [0, ±45, 90]$_s$ laminate having interlaminar filler

to the high intrinsic damping ability (tan δ) of the interlaminar filler material and its spherical shape. The spherical shape facilitates filler/matrix interfacial slippage during flexure of the composite specimen, particularly for the $[0]_8$ laminate for which slippage at the fibre/matrix interface is difficult. It is found by simple calculation that the interlaminar filler addition decreases the filler/matrix interface area per unit volume by 19% for the $[0]_8$ and $[90]_8$ laminates and by 13% for the $[0, \pm45, 90]_s$ laminate, but increases the filler/matrix interface area by 11% for the $[0]_8$ and $[90]_8$ laminates and by 10% for the $[0, \pm45, 90]_s$ laminate.

The main disadvantage of interlaminar filler addition is the density increase. The fractional increase in density is 34% for $[0]_8$ and $[90]_8$ and 26% for $[0, \pm45, 90]_s$. However, even when enhanced, the density (2·04 g cm^{-3}) remains much lower than that of the 2024–T4 Al–Cu alloy (2·71 g cm^{-3}). The 2024–T4 alloy is chosen for comparison because its tensile modulus (73 GN m^{-2}) is similar to the value of 74 GN m^{-2} for the storage flexural modulus of the $[0]_8$ laminate with the interlaminar filler. The ratio of loss modulus/density is 0·84 GN m^{-2}/g cm^{-3} for $[0]_8$ having interlaminar filler at 30°C and 1·0 Hz, compared with the corresponding value of <0·0063 GN m^{-2}/g cm^{-3} without interlaminar filler, and a value of 0·067 GN m^{-2}/g cm^{-3} for 2024–T4 alloy at 15 Hz.

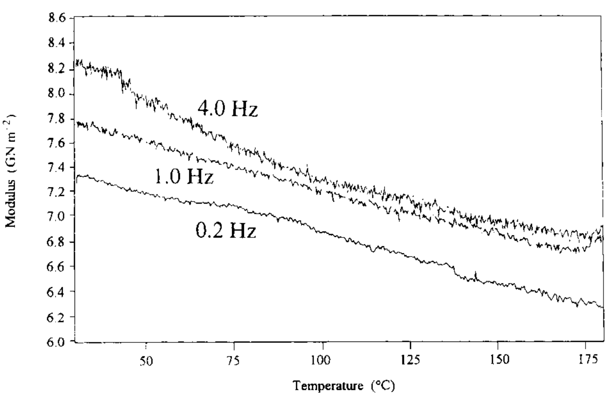

7 Plot of storage modulus *v.* temperature at 0·2, 1·0, and 4·0 Hz for [90]$_8$ laminate having interlaminar filler

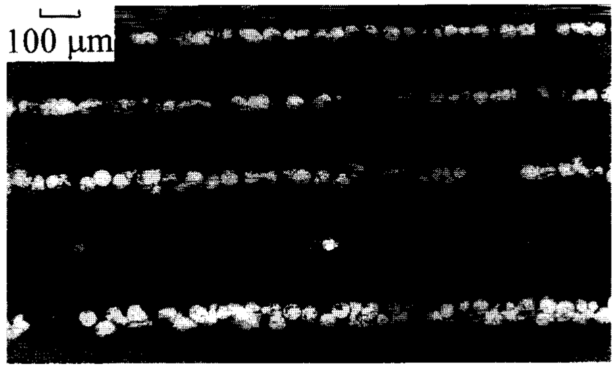

8 Optical micrograph of cross-section of [0, ±45, 90]$_s$ laminate having interlaminar filler

CONCLUSIONS

The addition of Sn–9Zn particles (25–45 µm in size) to a continuous carbon fibre epoxy matrix composite in the interlaminar region, such that the resulting composite contained 10 vol.-% particles (one monolayer between every two fibre plies) and 22–33 vol.-% fibres, produced a hybrid composite that exhibited a loss flexural modulus of 2 GN m^{-2} and a density of 2·0 g cm^{-3} for the $[0]_8$ laminate configuration. The particle addition increased the loss modulus by >20 000% and the density by 34%. The loss modulus increase was due to an increase in tan δ, which more than compensated for the decrease in the storage modulus. The particle addition decreased the loss modulus by 51–68% for the $[90]_8$ laminate configuration (except for certain combinations of temperature and frequency) owing to decreases in both tan δ and the storage modulus. The particle addition increased the loss modulus by >2900 to >14 000% for the $[0, \pm45, 90]_s$ laminate configuration owing to an increase in tan δ. The $[0]_8$ and $[0, \pm45, 90]_s$ laminate configurations are important practically, but the $[90]_8$ laminate configuration is not.

ACKNOWLEDGEMENT

This work was supported by US Department of Energy.

REFERENCES

1. J. FUJIMOTO, T. TAMURA, K. TODOME, and T. TANIMOTO: *J. Reinf. Plast. Compos.*, 1993, **12**, 738.
2. S. HE and M. D. RAO: *J. Compos. Mater.*, 1994, **28**, 112.
3. D. A. SARAVANOS and J. M. PEREIRA: *AIAA J.*, 1992, **30**, 2906.
4. K. NAKAO and Y. YAMASHITA: in 'Composites '86: Recent advances in Japan and the United States, Proc. Japan–US CCM–III', (ed. K. Kawata *et al.*), 743–750; 1986, Tokyo, Japan Society for Composite Materials.
5. B. Z. JANG, J. Y. LIAU, L. R. HWANG, and W. K. SHIH: *J. Reinf. Plast. Compos.*, 1990, **9**, 314–321.
6. M. NARKIS and E. J. H. CHEN: *SAMPE J.*, 1990, **26**, (3), 11–15.
7. S. FANG and D. D. L. CHUNG: *Composites*, 1990, **21**, (5), 419–424.
8. D. D. L. CHUNG: US Patent 5 091 242, 1992.